

## Structure and Catalytic Activity of $\text{MoO}_3 \cdot \text{SiO}_2$ Systems

### III. Mechanism of Oxidation of Propylene

N. GIORDANO

*Istituto di Chimica Industriale, Università di Messina, Messina, Italy*

M. MEAZZA, A. CASTELLAN, J. C. J. BART<sup>1</sup>

*Montedison Research Centre, 20021 Bollate, Milano, Italy*

AND

V. RAGAINI

*Istituto di Chimica Fisica, Università di Milano, Via Golgi 19, 20133 Milano, Italy*

Received July 20, 1976

The origin of the products of oxidation of propylene over the polymolybdic surface sites of an  $\text{MoO}_3 \cdot \text{SiO}_2$  catalyst has been correlated to the oxidation states of molybdenum by studying the effects of temperature (380–440°C),  $\text{O}_2/\text{C}_3\text{H}_6$  ratio (0.5–18), and dopants [ $\text{Zn(II)}$  and  $\text{Na(I)}$  ions] on overall conversion and selectivity in microreactor experiments, both in the presence and absence of steam. The selective oxidation product, acrolein, requires  $\text{Mo(VI)}$  active sites, as opposed to the other primary reaction product, acetaldehyde, and the by-products acetone, acetic acid, and propionaldehyde, which arise from interaction with  $\text{Mo(V)}$  and eventually  $\text{Mo(IV)}$  sites, respectively. Products of total oxidation,  $\text{CO}$  and  $\text{CO}_2$ , are formed over  $\text{Mo(VI)}$  active sites by consecutive reactions of the oxidized products mentioned or directly from propylene over  $\text{Mo(IV)}$  and  $\text{Mo(V)}$  sites in the case of  $\text{CO}_2$ . Propionaldehyde is indicated as a homogeneous reaction product.

#### 1. INTRODUCTION

A matter of considerable interest in investigations on the (amm)oxidation of olefins is the origin of by-products and the role of steam. This paper deals with some of these aspects in case of the  $\text{MoO}_3 \cdot \text{SiO}_2$  system. In previous papers (1, 2) we have discussed the relevant solid state characteristics of this system and the catalytic activity in the disproportionation and oxidation of propylene. Several forms of surface-bound oxomolybdenum species

have been identified; among these, the di- and polymolybdates account for both the selective and total oxidation of propylene, and only the former appear to be responsible for disproportionation of propylene to ethylene and butylenes (2).

We now aim at investigating the way polymolybdates control the oxidation of propylene; in particular, we attempt to elucidate the mechanism of formation of products such as acrolein (selective oxidation),  $\text{CO}$  and  $\text{CO}_2$  (total oxidation), and the by-products acetaldehyde, acetone, acetic acid, and propionaldehyde.

<sup>1</sup> Present address: Montedison G. Donegani Research Laboratories, Via del Lavoro 4, Novara, Italy.

## 2. EXPERIMENTAL

Samples of a 25 wt%  $\text{MoO}_3 \cdot \text{SiO}_2$  catalyst, activated at 500°C for 8 hr and further referred to as  $\text{MoO}_3\text{-25-500}$ , were prepared according to the methods of Ref. (1). Doped catalysts (25 wt%  $\text{MoO}_3$  + 1 wt%  $\text{NaOH}/74$  wt%  $\text{SiO}_2$  and 25 wt%  $\text{MoO}_3$  + 2 wt%  $\text{ZnO}/73$  wt%  $\text{SiO}_2$ ) were prepared in the same way after prior impregnation of  $\text{SiO}_2$  (Ketjen, type F-5) with aqueous solutions of  $\text{NaOH}$  or  $\text{Zn}(\text{NO}_3)_2 \cdot 6\text{H}_2\text{O}$  (BDH).

Catalytic activity experiments, either in the presence or absence of steam, were carried out in the flow microreactor of Ref. (3); to allow for stricter control of temperature, the microreactor was immersed in a bath of Sn-Pb alloy. Prior to use, the catalysts were conditioned in a flow of air, until attainment of the reaction temperature; afterwards, propylene was admitted in a prefixed air/propylene ratio (2.5–90), the total flow of reactants being constant (3.3 liter/h). Gas-chromatographic analysis and evaluation of results were made as before (3). After a 2-h run, the microreactor was bypassed and the

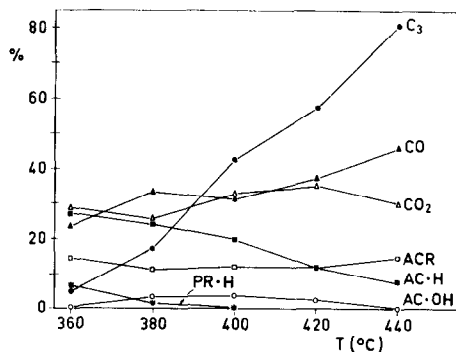


FIG. 1. Conversion of propylene and selectivities to products of oxidation over  $\text{MoO}_3\text{-25-500}$  as a function of the reaction temperature. Reaction conditions: feed ratio,  $\text{O}_2/\text{C}_3 = 2.4$ ; catalyst load, 2 ml;  $t_c$ , 1 s. Key: Conversion of propylene ( $\text{C}_3$ ),  $\bullet$ ; selectivity to acetaldehyde (AcH),  $\blacksquare$ ; acrolein (ACR),  $\square$ ; CO,  $\blacktriangle$ ;  $\text{CO}_2$ ,  $\triangle$ ; acetic acid (AcOH),  $\circ$ ; acetone (Ac),  $+$ ; propionaldehyde (PrH),  $*$ ; isopropyl alcohol (*i*-PrOH),  $\nabla$ .

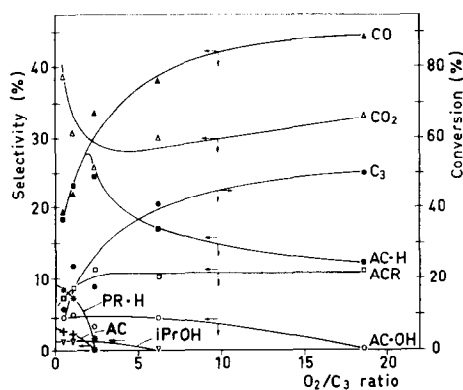


FIG. 2. Conversion of propylene and selectivities to products of oxidation over  $\text{MoO}_3\text{-25-500}$  as a function of the  $\text{O}_2/\text{C}_3$  ratio at 380°C;  $t_c = 1$  s. Symbols as in Fig. 1.

catalyst was extracted after rapid cooling to room temperature under a continuous stream of  $\text{N}_2$ . The spent catalyst was then analyzed by reflectance spectroscopy, ESR, and optical microscopy. Catalyst sampling was invariably performed in dry  $\text{N}_2$  atmosphere and contact with air was carefully avoided.

Diffuse reflectance spectra of the original and finely ground catalyst samples were recorded in the range of 240–1400 nm by use of a Perkin-Elmer Hitachi-EPS 3T spectrophotometer attachment against standards of  $\text{MgO}$ .

Optical microscopy measurements were carried out with a polarizing Ortholux Leitz microscope, with up to  $10^3\times$  magnification.

ESR measurements were made at room temperature with a JEOL JES ME 1X type spectrometer (X-band), using 100-kHz field modulation. The variations in spin concentration as a function of the temperature and  $\text{O}_2/\text{C}_3$  ratio were derived by comparison of the doubly integrated  $\text{Mo(V)}$  spectral intensities with the strong pitch Varian reference. To ensure that the ESR signal was proportional to the number of paramagnetic centers per unit volume, care was taken to fill the ESR sample

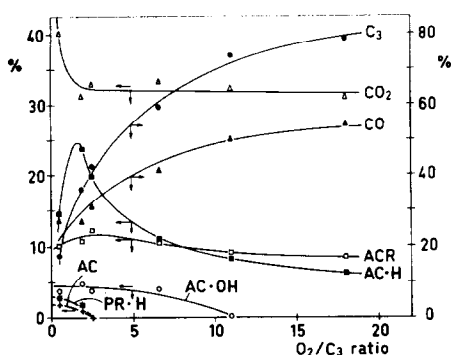


FIG. 3. Conversion of propylene and selectivities to products of oxidation over  $\text{MoO}_3\text{-25-500}$  as a function of the  $\text{O}_2/\text{C}_3$  ratio at  $400^\circ\text{C}$ ;  $t_c = 1$  s. Symbols as in Fig. 1.

tubes up to a height exceeding the depth of the resonant cavity.

### 3. RESULTS

#### 3.1 Catalytic Activity

Figure 1 shows the catalytic activity as a function of temperature, at fixed contact time (1 s) and  $\text{O}_2/\text{C}_3$  ratio (2.4). As evident, conversion increases steadily with temperature; selectivities to acrolein and  $\text{CO}_2$  remain almost constant, while CO increases as opposed to acetaldehyde. From the conversion of propylene and selectivities to various products (Figs. 2-4) as a function of the  $\text{O}_2/\text{C}_3$  ratio at different temperature levels ( $380^\circ$ ,  $400^\circ$  and  $440^\circ\text{C}$ ), it follows that: (i) The conversion of propylene always increases with increasing  $\text{O}_2/\text{C}_3$  ratio, especially in the range of  $\text{O}_2/\text{C}_3 = 1\text{-}5$ ; (ii) the selectivity to CO has a much similar behavior, in contrast to  $\text{CO}_2$ ; (iii) the selectivity to acrolein is almost insensitive to the  $\text{O}_2/\text{C}_3$  ratio, except at  $440^\circ\text{C}$  where a steady decrease is noted; (iv) acetaldehyde first increases up to a sharp maximum at  $\text{O}_2/\text{C}_3 = 2\text{-}1.5$  (at  $380$  and  $400^\circ\text{C}$ , respectively) and then decreases (at  $440^\circ\text{C}$  acetaldehyde behaves as acrolein); (v) all minor by-products (PrH, Ac, AcOH, and *i*-PrOH) share a limited stability range

( $\text{O}_2/\text{C}_3 = 18$  at  $380^\circ\text{C}$  and 11 at  $400^\circ\text{C}$ ) and are negligible at  $440^\circ\text{C}$ .

Table 1 compares the influence of steam with results of blank experiments performed under similar conditions. As evident, the conversion of propylene and the selectivities to  $\text{CO}_2$  are significantly lowered by addition of steam; on the contrary, the selectivities to acetaldehyde and acrolein remain almost unaffected. Sharp variations are displayed by acetone and acetic acid, which increase many times upon addition of steam.

The influence of solid dopants [ $\text{Na(I)}$  and  $\text{Zn(II)}$  ions were chosen in the expectation of neutralizing all acidic surface sites or at least part of them in a selective fashion] is illustrated in Table 2 and Figs. 5 and 6; the conversion of propylene is significantly lowered by both ions. The behavior of  $\text{Zn(II)}$  is illustrated in more detail in Fig. 5, as a function of the  $\text{O}_2/\text{C}_3$  ratio. Comparison with Fig. 3 indicates that addition of  $\text{Zn(II)}$  renders the selectivities almost independent of the  $\text{O}_2/\text{C}_3$  ratio and causes variations in the product distribution. The latter aspect is further illustrated in Fig. 6, where selectivities to acrolein and acetaldehyde of the doped samples are superimposed on those of the original catalyst as described in Ref. 2;

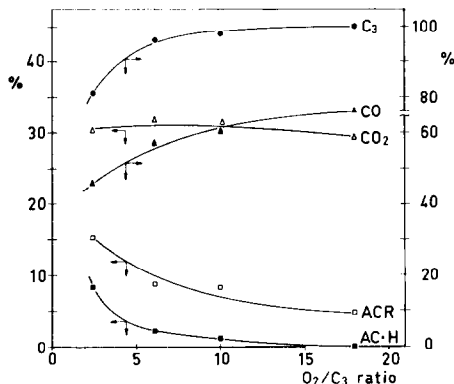


FIG. 4. Conversion of propylene and selectivities to products of oxidation over  $\text{MoO}_3\text{-25-500}$  as a function of the  $\text{O}_2/\text{C}_3$  ratio at  $440^\circ\text{C}$ ;  $t_c = 1$  s. Symbols as in Fig. 1.

at any conversion level, selectivities to acrolein are slightly higher in the case of doping by Zn(II) and Na(I). As to acetaldehyde, no appreciable variations are induced by Zn(II), as opposed to Na(I), which causes a substantial decrease.

### 3.2. Electron Spin Resonance

Results of ESR analysis are shown in Figs. 7–9 with reference to samples drawn from the microreactor following the experiments illustrated in Figs. 1–3, respectively. The intensity of the Mo(V) signal at  $g \cong 1.94(I_{\text{Mo}^{5+}})$  is a maximum at 380°C, whereas that due to products of cracking ( $I_C$ ,  $g = 2.003$ ) decreases regularly with temperature. At 380°C, the Mo(V) signal peaks at  $\text{O}_2/\text{C}_3 = 2.5$ , whereas  $I_C$  decreases with increasing  $\text{O}_2/\text{C}_3$  ratio; at 400°C both signals decrease as a function of the latter parameter.

### 3.3. Optical Reflectance Spectroscopy

Figure 10 shows spectra of a catalyst sample before and after use, indicating some differences, especially in the region of higher  $\lambda$ , i.e., where reduced forms of molybdenum are present (4). In fact, the absorbance at 950 nm originates from reduced heteropolyacids and/or polymolybdates containing both Mo(VI) and Mo(V) (cf. also Refs. 5 and 6). More particularly, the simultaneous occurrence of the shoulder at 600 nm and the absorption at 360 nm suggests the presence of a particular form of molybdenum blue, Mo<sub>4</sub>O<sub>10</sub>(OH)<sub>2</sub>, genotypic of MoO<sub>3</sub> and characterized by a

TABLE 1  
Influence of Steam on Catalytic Activity of MoO<sub>3</sub>-25-500 in the Oxidation of Propylene

	T = 380°C		T = 400°C	
	Blank	Steam	Blank	Steam
Selectivities				
CO	33.6	26.8	31.4	34.8
CO <sub>2</sub>	25.7	17.7	32.9	20.7
Acetaldehyde	24.6	24.1	19.8	19.7
Acrolein	11.3	10.5	12.2	13.0
Propionaldehyde	1.4	—	—	—
Acetone	—	7.0	traces	2.5
Acetic acid	3.4	13.9	3.7	9.3
Conversion of C <sub>3</sub> H <sub>6</sub> (%)	17.3	14.7	42.6	20.8
Sum of yields (%)	14.2	10.0	29.0	15.5
C <sub>3</sub> H <sub>6</sub> chemisorbed (%)	3.1	4.7	13.6	5.3
Conversion of O <sub>2</sub> (%)	15.0	10.4	55.5	19.5
CO <sub>2</sub> /CO	0.76	0.66	1.05	0.59

ratio Mo(VI)/Mo(V) = 1 and a square-pyramidal configuration (?). As evident from Fig. 10, some molybdenum blue is present even in the fresh catalyst.

Figure 11, which records spectra as a function of the  $\text{O}_2/\text{C}_3$  ratios (from 0.46 to 18) for runs at T = 400°C, shows that under more severe reducing conditions (lower  $\text{O}_2/\text{C}_3$  ratio) absorbance due to reduced species is higher; this holds not only for the 950-nm band of the Mo(V) fraction but also for the absorption around 500 nm, characteristic of Mo(IV) (cf. Ref. 6).

To derive a more quantitative correlation, the experimental values of absorbance for various catalysts have been expressed as  $(A/R)^{1/383}$ , according to the method of Doyle and Forbes (8), where  $R$  is the percentage of reflectance and  $A$

TABLE 2  
Influence of Doping on the Conversion (%) of Propylene over MoO<sub>3</sub>-25-500

Temperature (°C)	MoO <sub>3</sub> -25-500	MoO <sub>3</sub> -25-500 + 2 wt% ZnO	MoO <sub>3</sub> -25-500 + 1 wt% NaOH
400	40.0	25.1	—
420	57.8	39.7	—
440	80.8	—	29.0

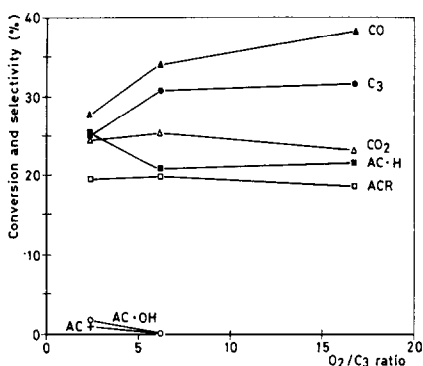


FIG. 5. Conversion of propylene and selectivities to products of oxidation over doped MoO<sub>3</sub>-25-500 (25 wt% MoO<sub>3</sub> + 2 wt% ZnO/73 wt% SiO<sub>2</sub>) as a function of the O<sub>2</sub>/C<sub>3</sub> ratio at 400°C;  $t_c = 1$  s. Symbols as in Fig. 1.

= (100 -  $R$ ). Taking the absorbance at  $\lambda = 950$  nm as representative of the Mo(V) fraction, the relative values of  $(A/R)^{1-388}$  are given in Fig. 12 as a function of the O<sub>2</sub>/C<sub>3</sub> ratio, at various temperature levels. At the lowest temperature (380°C), the  $A/R$  ratio passes through a maximum, whereas at other temperatures it decreases steadily with the increasing O<sub>2</sub>/C<sub>3</sub> ratio. Moreover, the higher the temperature and

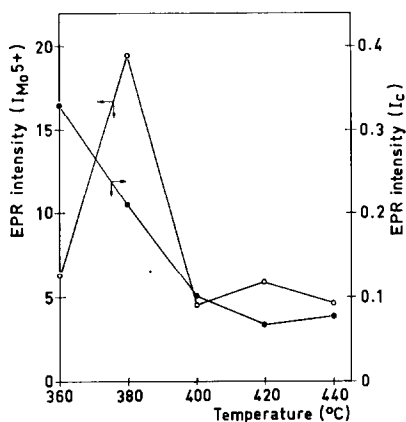


FIG. 7. Integrated ESR intensities of Mo(V) ( $I_{Mo^{5+}}$ ) and products of cracking ( $I_C$ ), as a function of the reaction temperature; O<sub>2</sub>/C<sub>3</sub> = 2.4.

O<sub>2</sub>/C<sub>3</sub> ratio, the more the electronic spectrum of the used catalyst approaches that of the fresh one (cf. Figs. 10 and 11); as mentioned above, the latter contains a small Mo(V) fraction.

### 3.4. Optical Microscopy

Two series of catalyst samples which differed in reaction conditions (O<sub>2</sub>/C<sub>3</sub> ratio and temperature) were investigated in the optical microscope. Catalyst samples after reaction at 400°C exhibit the darkest coloration (i.e., are more strongly reduced) at the lowest O<sub>2</sub>/C<sub>3</sub> ratios and are covered with carbonaceous material, impeding further detailed observation. The reduction phenomena mainly involve the surface layers; in the more strongly reduced samples we notice a more extensive formation of MoO<sub>3</sub> clusters, as particularly evident in the case of treatment with O<sub>2</sub>/C<sub>3</sub> = 6.6. However, it does not result that the whiskers are reduced. Rather, the reduced species are almost insoluble in H<sub>2</sub>O and soluble in 32% NH<sub>4</sub>OH. The residues of leaching with NH<sub>4</sub>OH, which probably contain silicomolybdic acid-like species, show no reductive phenomena.

Similar observations were made for a series of catalysts subjected to different

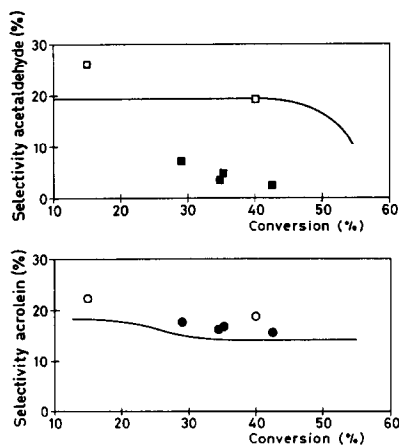


FIG. 6. Selectivities to acetaldehyde and acrolein as a function of the conversion of propylene over an MoO<sub>3</sub>-25-500 catalyst (smooth curve), as compared to the Zn(II)- ( $\square$ ,  $\circ$ ) and Na(I)- ( $\blacksquare$ ,  $\bullet$ ) doped samples;  $T_R = 440^\circ\text{C}$ , feed ratio O<sub>2</sub>/C<sub>3</sub> = 2.4,  $t_c = 1$  s.

reaction temperatures (360 to 440°C) at constant  $\text{O}_2/\text{C}_3$  ratio (2.5); the  $\text{NH}_4\text{OH}$ -leached residue shows minor reducibility at temperatures exceeding 400°C, whereas the  $\text{MoO}_3$  cluster formation could not be correlated with temperature but rather seems to be a function of the  $\text{O}_2/\text{C}_3$  ratio.

#### 4. DISCUSSION

Comparison of the catalytic activity patterns (Figs. 2-4) with optical reflectance data (Fig. 12) and ESR results (Figs. 8 and 9) reveals some close correlations. In particular, the conversion of propylene always decreases as the  $\text{Mo(V)}$  concentration increases; an exception is the behavior of  $(A/R)^{1-383}$  and  $I_{\text{Mo}^{5+}}$  for samples treated with an oxygen-poor reagent flow ( $\text{O}_2/\text{C}_3$  ratio  $< 3$ ) at 380°C. The result implies that the conversion of propylene increases with a higher concentration of  $\text{Mo(VI)}$  active sites, in agreement with the results of Sancier *et al.* (9) for  $\text{MoO}_3 \cdot \text{SiO}_2$  as well as for  $\text{MoO}_3 \cdot \text{Bi}_2\text{O}_3$ . The significant effect of the  $\text{O}_2/\text{C}_3$  ratio on the conversion of propylene implies a relationship between the valence states of molybdenum, as expressed by the  $\text{Mo(VI)}/\text{Mo(V)}$

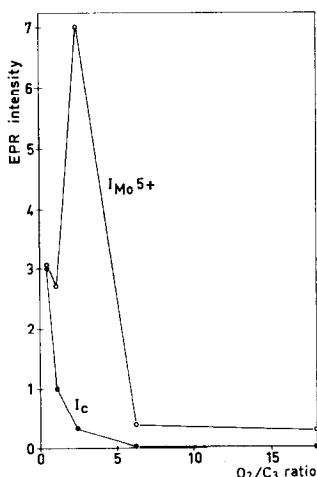


FIG. 8. Integrated ESR intensities of  $\text{Mo(V)}$  ( $I_{\text{Mo}^{5+}}$ ) and products of cracking ( $I_c$ ), as a function of the  $\text{O}_2/\text{C}_3$  ratio;  $T = 380^\circ\text{C}$ .

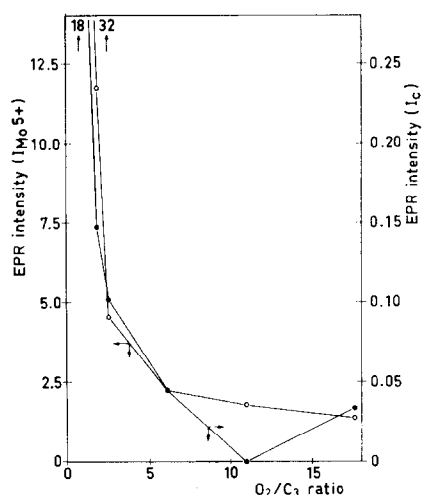
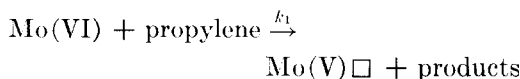
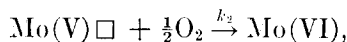


FIG. 9. Integrated ESR intensities of  $\text{Mo(V)}$  ( $I_{\text{Mo}^{5+}}$ ) and products of cracking ( $I_c$ ), as a function of the  $\text{O}_2/\text{C}_3$  ratio;  $T = 400^\circ\text{C}$ .

ratio and the concentration of the reagents. Thus, if we consider the reduction



and the reoxidation step



then, under steady-state conditions, the following relationship holds:

$$\text{Mo(VI)}/\text{Mo(V)} = (k_2[\text{O}_2]^2)/k_1[\text{C}_3],$$

which is qualitatively in agreement with

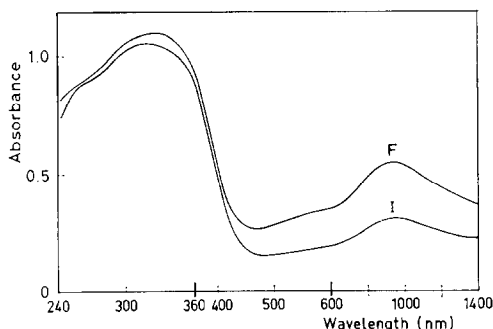


FIG. 10. Optical reflectance spectra of  $\text{MoO}_3$ -25-500 before (I) and after (F) oxidation of propylene ( $T = 400^\circ\text{C}$ ;  $\text{O}_2/\text{C}_3 = 11$ ;  $t_c = 1$  s).

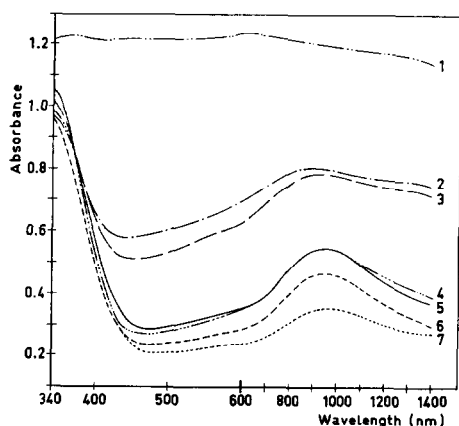


Fig. 11. Optical reflectance spectra of  $\text{MoO}_3$ -25-500 after oxidation of propylene ( $T = 400^\circ\text{C}$ ;  $t_o = 1$  s) at various  $\text{O}_2/\text{C}_3$  ratios: 0.5 (1), 1.8 (2), 2.5 (3), 6.6 (4), 11 (5), 18 (6), and fresh catalyst (7).

the experimentally found values. In practice, the net effect of a higher  $\text{O}_2/\text{C}_3$  ratio is to increase the  $\text{Mo(VI)}$  fraction at the expense of  $\text{Mo(V)}$ , at any temperature level. On the other hand, a decrease of temperature generally corresponds to an increase of  $\text{Mo(V)}$  (Fig. 7), causing the reduction step to become more controlling at the expense of the reoxidation. This behavior is easily noticed by comparing the results of ESR (Figs. 8 and 9) and optical reflectance (Fig. 12); an exception to the general behavior is the  $A/R$  ratio at  $380^\circ\text{C}$

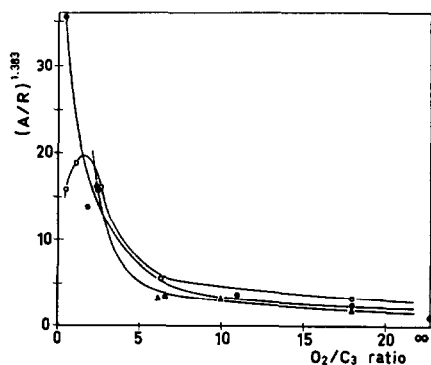


Fig. 12. Plot of  $(A/R)^{1.383}$ , measured at  $\lambda = 950$  nm, as a function of the  $\text{O}_2/\text{C}_3$  ratio for  $\text{MoO}_3$ -25-500, after oxidation of propylene at  $380^\circ\text{C}$  ( $\circ$ ),  $400^\circ\text{C}$  ( $\bullet$ ), and  $440^\circ\text{C}$  ( $\blacktriangle$ );  $t_o = 1$  s.

in Fig. 12, which passes through a maximum at the lowest  $\text{O}_2/\text{C}_3$  ratio. Under the latter conditions, the reduction of  $\text{Mo(VI)}$  may exceed the formation of  $\text{Mo(V)}$ , thus causing the onset of some  $\text{Mo(IV)}$  species. Similarly, in Fig. 7 the lowest value of the ESR signal for the  $360^\circ\text{C}$  catalyst might simply be due to an excess of  $\text{Mo(IV)}$  with respect to  $\text{Mo(V)}$ , with the former giving no paramagnetic signal. Altogether, within the range of experimental conditions investigated, we are dealing chiefly with  $\text{Mo(VI)}$  and  $\text{Mo(V)}$ , the former in increasing concentration at higher temperature.

As is evident from the experimental results, not only the catalytic activity, but also the selectivities to various products are strongly dependent upon the  $\text{Mo(VI)}/\text{Mo(V)}$  ratios. It appears safe to conclude that a close relationship exists between  $\text{Mo(V)}$  and acetaldehyde formation. Comparison of Figs. 2-4 with Figs. 8, 9, and 12 indicates a parallelism between the decrease of acetaldehyde and  $\text{Mo(V)}$ ; a notable exception is the behavior at  $\text{O}_2/\text{C}_3$  ratios  $\leq 2.5$  (at  $380$  and  $400^\circ\text{C}$ ), where acetaldehyde goes through a maximum. From arguments discussed before, it appears that in this region some  $\text{Mo(IV)}$  was formed, causing an unbalance in the reaction rates. Apparently, parallel or consecutive reactions compete with or consume acetaldehyde. On the basis of the experimental results (Figs. 2-4), the secondary reaction product is likely to be  $\text{CO}_2$ . In fact,  $\text{CO}_2$  and acetaldehyde show an opposite behavior, suggesting that more propylene is converted directly into  $\text{CO}_2$  or that acetaldehyde is oxidized to  $\text{CO}_2$  by  $\text{Mo(V)}-\text{Mo(IV)}$  sites ( $\text{O}_2/\text{C}_3 < 2.5$ ).

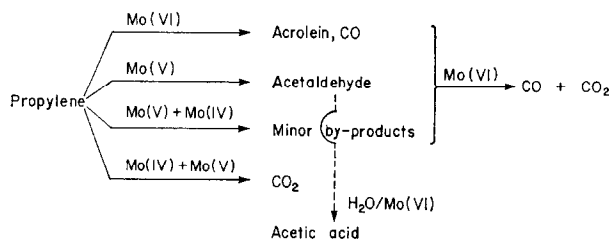
As to the formation of  $\text{CO}$ , Figs. 2-4 show this product to be strongly related to  $\text{Mo(VI)}$ , even though we cannot distinguish whether it originates directly from propylene or from other oxidized molecules. On the assumption that the observations of Gorshkov *et al.* (10, 11) are valid also

in our case, at least part of CO may originate from consecutive oxidation of acrolein. This would explain the invariance or decrease of acrolein at higher Mo(VI) levels, contrary to the expectation based upon the results of Sancier *et al.* (9) and our previous work on the ammoxidation of propylene (12). The result is rationalized if we remember that acrolein is more reactive than acrylonitrile and is readily oxidizable due to the double bond in conjugation with the carbonyl group. By extension of our present experiments over a wider range of variables (i.e., different contact times at the various  $\text{O}_2/\text{C}_3$  ratios), a more complete set of results may be derived along the lines of our previous work on the ammoxidation of propylene (12). As stated there, acrylonitrile is strongly related to Mo(VI), in accordance with other work (13). On the basis of available literature and by analogy with the am-

moxidation reaction, it may be assumed that acrolein is related to the Mo(VI) fraction, although the exact dependency cannot be given at present.

With regard to all minor by-products, the results strongly suggest that they are probably related to Mo(V); however, as at low  $\text{O}_2/\text{C}_3$  ratios Mo(IV) is present, these sites may also play a role (Figs. 2-4). Anyway, whether related to Mo(V) or Mo(IV), all minor by-products (*i*-PrOH, Ac, AcOH, PrH) always decrease with increase of temperature and  $\text{O}_2/\text{C}_3$  ratio, reaching negligible values under the most severe conditions. Obviously, the observed decay of minor by-products under these conditions may partly be attributed to consecutive reactions over Mo(VI).

Combining the observations, the following tentative scheme may then be derived, constituting the basis for some mechanistic considerations:

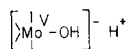


The dependence of acrolein upon Mo(VI) proves the assumption that propylene is adsorbed on the cation with the highest valence, as agreed for mixed oxides (14-20). Indeed, in the oxidation reaction of propylene, Mo(VI) in molybdates or Sb(V) in antimony-based oxides are claimed as the sites of catalytic attack through the well-established mechanism involving H-abstraction and formation of  $\pi$ -allyl complexes (21, 22). At variance with mixed oxides, the  $\text{MoO}_3 \cdot \text{SiO}_2$  system lacks the presence of an auxiliary cation such as Bi(III), Sn(IV), Fe(III) capable of reoxidizing the principal cation and leading to transfer of electrons to the molecular oxygen. The inability of  $\text{SiO}_2$  to act as an oxidizing

agent is beyond doubt. This characteristic explains the poor selectivities to acrolein over  $\text{MoO}_3 \cdot \text{SiO}_2$  as compared to mixed oxide catalysts, as well as the high  $\text{O}_2/\text{C}_3$  ratios needed to provide complete reoxidation of the catalyst. On the same grounds the wide range of existence of Mo(V) and its high contribution to the formation of by-products can be understood. The simplest of these reactions is the addition of a proton to form the isopropyl carbocation which may be converted into acetone, by hydration or by reaction with an anion of the lattice, followed by dehydrogenation. Hydroxyl groups and protons on the surface of the catalyst and notably on the oxidation site are more or less perma-



nent species, as they are formed from water during the oxidative dehydrogenation process itself. The risk of secondary reactions induced by these species (protons and hydroxyl groups) can be minimized only if dehydration of oxidation sites is rapid and efficient. Protonic and hydroxyl groups and consequently dehydration rates can be profoundly modified by the nature of the oxidation sites. Thus, increased Brønsted acidity is to be expected on going from Mo(VI) to Mo(V); correspondingly, as discussed in a previous paper (23), the formation of a complex like



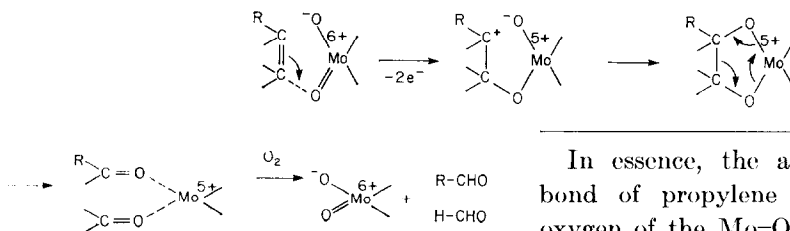
is suggested on which propylene is more strongly adsorbed than in the analogous Mo(VI) complex. This situation should favor formation of carbocations, hence of isopropoxy intermediates, interfering with the allylic route. Changes in the valency of molybdenum also affect the reactivity of the OH groups in the sense of an increasing mobility on going from Mo(VI) to Mo(V). Namely, as the heat of hydration on metal cations decreases strongly with decreasing charge of the cation, Mo(V) should dissociate its water ligand faster than Mo(VI) and lead to a higher rate of desorption of the ultimate products of reaction, i.e., *i*-PrOH and acetone. Generally speaking, reactions of this type attain increasing significance at lower temperature, following favorable changes in the hydration and protonation equilibria of the catalyst and the olefin. This is coherent with the experimental results and explains also the favorable effect of water added back (see Table 1), especially in the case of

acetone. Lack of sensitivity for isopropyl alcohol is accounted for by the low equilibrium of the simplest hydration reaction.

Among the by-products, acetaldehyde occupies a relevant place, being the second largest product observed. Its formation may be accounted for simply by the addition to acrolein of a molecule of water (or, eventually, of a hydroxyl group of the active site) to form  $\beta$ -hydroxypropionaldehyde (24), which can easily be oxidized or dissociated to form formaldehyde and acetaldehyde by retroaldolization (25). However, from Fig. 6 it seems likely that this possibility, although valid under other reaction conditions, is not pertinent to our case, as acetaldehyde is a primary reaction product together with acrolein; both products reach a high value at the lowest propylene conversion levels. Therefore, the possibility of an electrophilic attack on the double bond of propylene seems to be the more appropriate to our results; this is especially true in the presence of Mo=O oxidizing groups with a certain degree of polarity. Looking at experimental results favoring a relationship between acetaldehyde and Mo(V), we propose that Mo=O or Mo-OH groups on Mo(V) structures



might have such a property. In fact, taking as a model the mechanisms established for oxidation in the homogeneous phase, we can envisage a process in accordance with the following scheme, formerly proposed by Weiss *et al.* (26):



In essence, the attack on the double bond of propylene by the electrophilic oxygen of the Mo=O group is followed by

cyclization and fragmentation of the cyclic structure into two carbonyl compounds (acetaldehyde and formaldehyde), and, subsequently, by the complete oxidation of a large fraction of the latter. In fact, both CO and  $\text{CO}_2$  increase as acetaldehyde reaches a maximum as a function of increasing  $\text{O}_2/\text{C}_3$  ratios; in other words, formaldehyde and acetaldehyde are readily oxidized, possibly through Mo(VI). An open possibility is still that acetaldehyde is further oxidized to acetic acid under the influence of water (Table 1); this path involves dehydrogenation of the aldehyde group to form an acylium ion, which reacts with an oxygen anion from the lattice (27) to yield a carboxylate anion.

The role of acidic sites in the formation of acetaldehyde is also evident from the negative effect of the Na-dopant on the selectivity (Fig. 6); Zn(II) clearly acts differently and influences the oxidation rates instead of neutralizing acidic sites.

The last of the series of by-products, propionaldehyde, deserves special attention. Its origin cannot be attributed to a carbocation mechanism, as it contradicts the Markownikow rule. The possibility of propionaldehyde being formed by the lowest reduced molybdenum species, Mo(IV), cannot be ruled out, but so far lacks a simple mechanistic scheme. The considerable diversity from other by-products, in terms of selectivity as a function of the  $\text{O}_2/\text{C}_3$  ratios, suggests that propionaldehyde belongs to products of homogeneous reactions either through a primary route or as a result of consecutive isomerization of propylene oxide. In fact, the latter product is commonly indicated among products of homogeneous reactions, together with propionaldehyde (28, 29).

## 5. CONCLUSIONS

The origin of the products of oxidation and ammoxidation of propylene over molyb-

dena catalysts indicates close relationships, in particular with regard to the formation of acrolein and acrylonitrile over Mo(VI) active sites and of acetaldehyde and acetonitrile over Mo(V) species; the latter also account for most other by-products. The main difference between the two reactions is found in the origin of the products of total oxidation, CO and  $\text{CO}_2$ .

## ACKNOWLEDGMENTS

One of us (M.M.) is indebted to Montedison S.p.A. for a research fellowship, during the tenure of which this work was performed.

## REFERENCES

1. Castellan, A., Bart, J. C. J., Vaghi, A., and Giordano, N., *J. Catal.* **42**, 162 (1976).
2. Vaghi, A., Castellan, A., Bart, J. C. J., Giordano, N., and Ragaini, V., *J. Catal.* **42**, 381 (1976).
3. Giordano, N., Padovan, M., Vaghi, A., Bart, J. C. J., and Castellan, A., *J. Catal.* **38**, 1 (1975).
4. Giordano, N., Castellan, A., Bart, J. C. J., Vaghi, A., and Campadelli, F., *J. Catal.* **37**, 204 (1975).
5. Mitchell, P. C. H., and Trifirò, F., *J. Chem. Soc. (A)*, 3183 (1970).
6. Porter, V. R., White, W. B., and Roy, R., *J. Solid State Chem.* **4**, 250 (1972).
7. Wilhelmi, K. A., *Acta Chem. Scand.* **23**, 419 (1969).
8. Doyle, W. P., and Forbes, F., *Anal. Chim. Acta* **33**, 108 (1965).
9. Sancier, K. M., Dozono, T., and Wise, H., *J. Catal.* **23**, 270 (1971).
10. Gorshkov, A. P., Isagulyants, G. V., Derbentsev, Yu. I., Margolis, L. Ya., and Kolchin, I. K., *Dokl. Akad. Nauk SSSR* **186**, 827 (1969).
11. Gorshkov, A. P., Kolchin, I. K., Gribov, A. M., and Margolis, L. Ya., *Kinet. Katal.* **9**, 1086 (1968).
12. Giordano, N., and Bart, J. C. J., *Rec. Trav. Chim.* **94**, 28 (1975).
13. Cathala, M., and Germain, J. E., *Bull. Soc. Chim. Fr.* **11**, 4114 (1970).
14. Batist, P. A., Kapteijns, C. J., Lippens, B. C., and Schuit, G. C. A., *J. Catal.* **7**, 33 (1967).
15. Peacock, J. M., Parker, A. J., Ashmore, P. G., and Hockey, J. A., *J. Catal.* **15**, 373 (1969).
16. Peacock, J. M., Parker, A. J., Ashmore, P. G., and Hockey, J. A., *J. Catal.* **15**, 387 (1969).

17. Peacock, J. M., Parker, A. J., Ashmore, P. G., and Hockey, J. A., *J. Catal.* **15**, 398 (1969).
18. Peacock, J. M., Sharp, M. J., Parker, A. J., Ashmore, P. G., and Hockey, J. A. *J. Catal.* **15**, 379 (1969).
19. Margolis, L. Ya., *Advan. Catal.* **14**, 430 (1963).
20. Godin, G. W., McCain, C. C., and Porter, E. A., in "Proceedings of the Fourth International Congress on Catalysis (Moscow, 1968)," Vol. I, p. 271. Akademiai Kiadó, Budapest, 1971.
21. Germain, J. E., "Catalytic Conversion of Hydrocarbons," p. 231. Academic Press, New York, 1969.
22. Adams, C. R., and Jennings, T. J., *J. Catal.* **3**, 549 (1964); **2**, 63 (1963).
23. Giordano, N., Vaghi, A., Bart, J. C. J., and Castellan, A., *J. Catal.* **38**, 11 (1975).
24. Hall, R. H., and Stern, E. S., *J. Chem. Soc.* 490 (1950).
25. Schulz, H., and Wagner, H., *Angew. Chem.* **62**, 105 (1950).
26. Weiss, F., Marion, J., Metzger, J., and Cognion, J. M., *Kinet. Katal.*, **14**, 45 (1973).
27. Sachtler, W. M. H., *Catal. Rev.* **4**, 27 (1970).
28. Bayer, A. G., British Patent 960,332 (June 10, 1964).
29. Daniel, C., Monnier, J. R., and Keulks, G. W., *J. Catal.* **31**, 360 (1973).